Available online at www.sciencedirect.com

ScienceDirect

Procedia CIRP 62 (2017) 209 – 214

www.elsevier.com/locate/procedia

10th CIRP Conference on Intelligent Computation in Manufacturing Engineering - CIRP ICME '16

Dry turning of Ti6Al4V: tool wear curve reconstruction based on cognitive sensor monitoring

Alessandra Caggiano[a,b], Francesco Napolitano[a,c,*], Roberto Teti[a,c]

[a]*Fraunhofer Joint Laboratory of Excellence on Advanced Production Technology (Fh-J_LEAPT), Naples, Italy*
[b]*Dept. of Industrial Engineering, University of Naples Federico II, P.le Tecchio 80, 80125 Naples, Italy*
[c]*Dept. of Chemical, Materials and Industrial Production Engineering, University of Naples Federico II, P.le Tecchio 80, 80125 Naples, Italy*

* Corresponding author. Tel.: +39-081-7682371; fax: +39-081-7682362. *E-mail address:* francesco.napolitano4@unina.it

Abstract

Dry turning of Ti6Al4V alloy is a hard process due to the low thermal conductivity and flexibility of this difficult-to-machine material, generating very high temperatures in both workpiece and tool cutting edge, rapid tool wear and high vibrations during machining. The use of coolants offers the advantage to reduce the high process temperatures, but is not suitable in a green technology perspective due to its high environmental impact. With the aim to allow for dry turning of Ti6Al4V alloy, monitoring of tool wear during the process is required. To achieve this goal, a cognitive sensor monitoring procedure based on the acquisition and processing of force, acoustic emission and vibration sensor signals is implemented, allowing for an accurate tool wear curve reconstruction.

Peer-review under responsibility of the scientific committee of the 10th CIRP Conference on Intelligent Computation in Manufacturing Engineering
Keywords: Sensor monitoring; Titanium alloy; Dry turning; Tool wear

1. Introduction

In the last few years, manufacturing industries are facing new challenges related to sustainability of their operations, with particular reference to energy and resource efficiency improvement and environmental impact reduction [1]. These goals are particularly challenging when dealing with machining of difficult-to-machine materials such as titanium alloys, requiring extensive use of lubricant and coolant fluids which are undesirable in a green technology perspective.

Within the aerospace industry, Ti6Al4V is probably the most widespread titanium alloy, displaying very high tensile strength and toughness at high temperatures combined with low density. The mechanical and thermal properties of Ti6Al4V are reported in Table 1 [2]. This alloy has the same tensile strength of steel being 45% lighter, a modulus of elasticity 50% lower than steel, and a very low thermal conductivity (down to 1/5 of steel). Moreover, an allotropic transformation occurs in the titanium structure at 882 °C (beta transus), with change from alpha titanium (EC structure) to the more deformable beta titanium (CCC structure) [2-3].

Because of the material properties described above, two critical issues arising during turning of Ti6Al4V alloy cylindrical parts are represented by taper and excessive vibrations due to bar inflection and the very high temperatures in the workpiece and at the tool cutting edge (~ 1100°C) due to the material low thermal conductivity. These phenomena are intensified when turning under dry conditions, as the high temperatures in the cutting zone cause rapid tool wear and changes in the workpiece structure close to the cut zone [4-7].

With the aim to allow for dry turning of Ti6Al4V alloy, monitoring and on-line diagnosis of tool wear state during the process is required. To achieve this goal, a cognitive sensor monitoring procedure based on the acquisition and processing of cutting force, acoustic emission and vibration signals during turning is implemented. The developed procedure based on sensor signal feature extraction, selection and cognitive pattern recognition via artificial neural networks allows for an accurate diagnosis on tool wear state [8-15]. This diagnosis can be used for tool replacement strategies based on actual tool wear state instead of preventive strategies, allowing to fully exploit the entire tool life [14].

Peer-review under responsibility of the scientific committee of the 10th CIRP Conference on Intelligent Computation in Manufacturing Engineering
doi:10.1016/j.procir.2017.03.046

Table 1. Comparison between main properties of Ti6Al4V and steel.

Properties	Ti6Al4V	Steel
Density (g/cm^3)	4.43	7.86
Melting point (°C)	1649	1454
Thermal conductivity (W/mK)	7.2	11.2-36.7
Elastic modulus (GPa)	114	210
Tensile strength, ultimate (MPa)	1000	827
Tensile strength, yield (MPa)	880	552

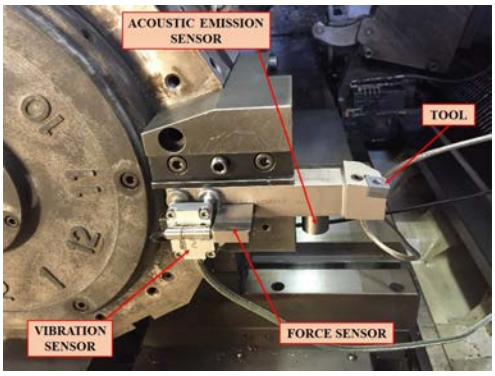

Fig. 1. Multiple sensor system mounted on the tool holder.

2. Experimental testing campaign

2.1. Experimental setup

The experimental testing campaign consists of consecutive cylindrical turning passes of 100 mm length under different cutting conditions on 60 mm diameter Ti6Al4V alloy bars.

The CNC lathe is equipped with a multiple sensor system (Fig. 1) including a Montronix FS1xCXK-x-ICA 3D force sensor, a Montronix BV100 acoustic emission sensor and a Montronix Spectra Pulse 3D vibration sensor. The first two sensors, providing analog signals, are connected to a NI USB-6361 DAQ board for digitization and acquisition on PC of the three cutting force components (F_x, F_y, F_z) and the Root Mean Square of acoustic emission (AE_{RMS}) signals. The 3D vibration sensor is a digital wireless sensor which acquires and sends to the PC the sensorial data corresponding to the three vibration acceleration components (A_x, A_y, A_z).

The DAQ board allows to set the signal sampling rate; following the Nyquist-Shannon sampling theorem, 10 kS/s was selected as a sufficient sampling rate to allow capturing all the original signal information. On the other hand, the digital vibration acceleration sensor directly carries out the signal sampling with a fixed rate of 3.24 kS/s.

2.2. Tool and machining parameters

The cutting tool employed during the experimental turning tests is a Mitsubishi CNMG120404-MS MT9015 turning insert. It is an uncoated tungsten carbide tool, specific for titanium machining and suitable for medium material removal conditions, with ISO S15 carbide grade composition.

Table 2. Cutting conditions employed in the experimental campaign.

Parameter	Minimum	Intermediate	Maximum
Cutting speed (m/min)	60	70	80
Feed rate (mm/rev)	0.10	0.25	0.30
Depth of cut (mm)	0.5	1.0	1.5

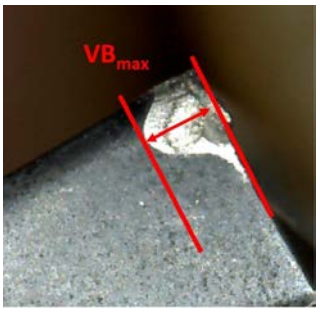

Fig. 2. Measurement of maximum flank wear land, VB_{max}.
Cutting parameters: v = 60 m/min, f = 0.3 mm/rev, d = 1 mm.

A full factorial experimental design was applied for turning tests: three factors corresponding to the cutting parameters, i.e. cutting speed, v, feed rate, f, and depth of cut, d, were taken into consideration, and three different levels of each factor were tested according to the experimental plan in Table 2.

The testing procedure was planned in accordance with the requirements indicated by the standard on tool-life testing with single-point turning tools (ISO 3685:1993).

3. Tool wear development

The final aim of this work is to find correlations between the multiple sensor signals acquired during dry turning of Ti6Al4V and the tool wear conditions. In order to measure tool wear during the turning tests, after each turning pass a magnified picture of the cutting edge was acquired through a portable digital microscope (DINO-LITE Premier) and the maximum flank wear land, VB_{max}, was measured (Fig. 2). The criterion for the end of tool life was established by setting a 0.6 mm threshold for the highest acceptable VB_{max} value.

The results on tool wear development confirm that cutting speeds 70 m/min and 80 m/min are too high for dry turning of Ti6Al4V. As a matter of fact, by increasing the cutting speed, a large increase in tool wear rate and a notable reduction of machining time and material removal carried out with a single tool are observed (Fig. 3). As regards the differences between tool wear development at 60 m/min and 70 m/min, they are smaller at low feed rate and depth of cut, but significantly increase with growing feed rate and depth of cut.

On the basis of the experimental results, 60 m/min appears as the most suitable value for maximum cutting speed in dry turning of Ti6Al4V. By setting the cutting speed at 60m/min, the influence of depth of cut or feed rate variations can be observed in Figs. 4-5. A notable growth of tool wear rate (3 times faster) is found when increasing depth of cut from d_1 = 0.5 mm to d_2 = 1 mm and d_3 = 1.5 mm as well as when increasing feed rate from f_2 = 0.25 mm/rev to f_3 = 0.3 mm/rev.

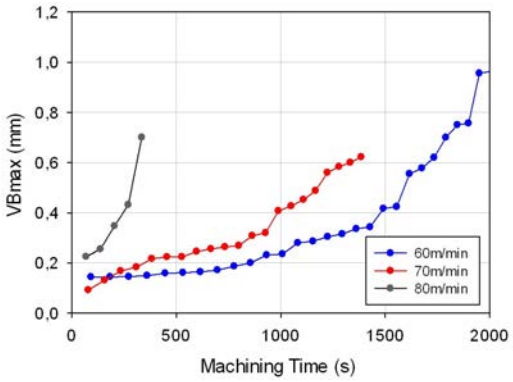

Fig. 3. Measured tool flank wear values vs machining time for v_1 = 60 m/min, v_2 = 70 m/min, v_3 = 80 m/min (f = 0.2 mm/rev, d = 0.5mm).

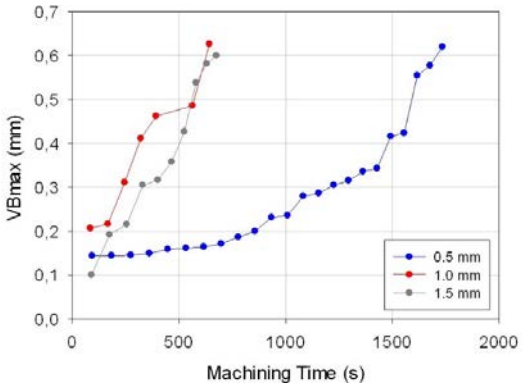

Fig. 4. Measured tool flank wear values vs machining time for d_1 = 0.5 mm, d_2 = 1 mm, d_3 = 1.5 mm (v = 60 m/min, f = 0.2 mm/rev).

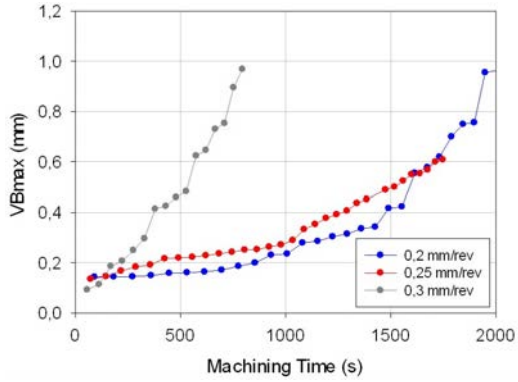

Fig. 5. Measured tool flank wear values vs machining time for f_1 = 0.2 mm/rev, f_2 = 0.25 mm/rev, f_3 = 0.3 mm/rev (v = 60 m/min, d = 0.5 mm).

4. Signal processing and analysis

4.1. Signal segmentation and resampling

The sensor signals acquired by the multiple sensor system during the experimental turning tests included head and tail transient portions which do not belong to the actual machining process. As these signal portions are not relevant for process monitoring, they had to be removed in order to consider only the signal part consistent with steady state machining [8-9].

This signal segmentation procedure was carried out using two different methods for the DAQ board signals (F_x, F_y, F_z and AE_{RMS}) and for the vibration acceleration digital sensor signals (A_x, A_y, A_x), respectively.

As regards the DAQ board signals, segmentation was performed on the basis of the F_x signal and synchronically extended to the other signals F_y, F_z and AE_{RMS}. The automated segmentation procedure to cut out transient signal portions is based on the calculation of the signal moving average with a fixed subset size of 50 samples to reduce high frequency oscillations. The mean value of the resulting smoother signal is then employed as a threshold to identify the steady signal portion. In particular, considering only the signal portion over this threshold, the slope between consecutive samples is calculated: the first sample with negative slope and the last sample with positive slope are identified as the start and the end of the segmented signal (Fig. 6). The segmented signals are shown in Figs. 7-8.

A different segmentation procedure was applied to the acceleration signals acquired by the digital vibration sensor. Each vibration acceleration component signal (A_x, A_y, A_z) has an offset which depends on its orientation with respect to the gravity acceleration (the sum of the x, y and z offset values is 9.81 m/s^2). These signals are symmetric around their offset value, so the developed procedure identifies the difference between transient and steady state signal portions by calculating the square of the signal, i.e. the square of the vertical distance of the signal values from the rest state. The first and the last value over the threshold set at 20 m/s^2 are selected as the start and the end of the signal segment consistent with actual machining. Moreover, a resampling of the digital sensor signals to 10 KS/s was necessary. As a matter of fact, the digital vibration acceleration signals were compulsorily acquired with a fixed sampling rate of 3.24 kS/s, whereas the DAQ signals were acquired with a properly chosen sampling rate of 10 kS/s. The final segmented vibration acceleration signals are shown in Fig. 9.

4.2. Sensor signal features extraction

Signal pre-processing was carried out to isolate the relevant signal portion with the aim to allow for the subsequent extraction of functional sensor signal features correlated with tool state and/or process condition [8].

A statistical approach in the time domain was applied for feature extraction. Among the several statistical signal features that can be extracted from a time domain signal, the following five were taken into consideration: arithmetic mean, variance, skewness, kurtosis and signal power.

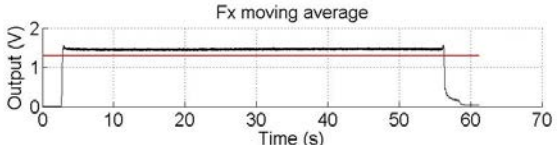

Fig. 6. Moving average of F_x cutting force component signal and set threshold (red line).

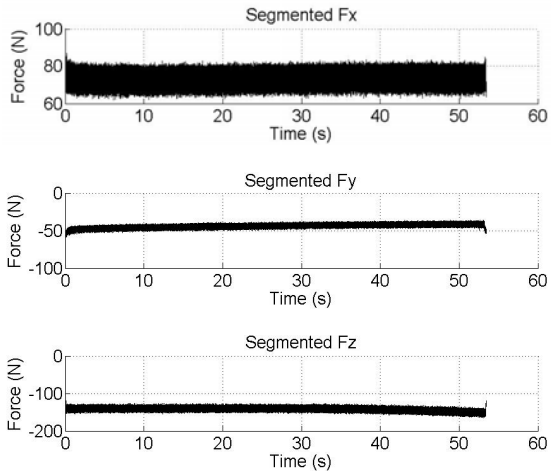

Fig. 7. Segmented F_x, F_y, F_z cutting force components signals.

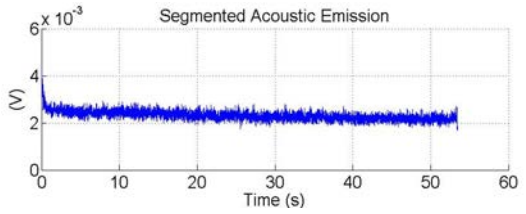

Fig. 8. Segmented acoustic emission RMS signal.

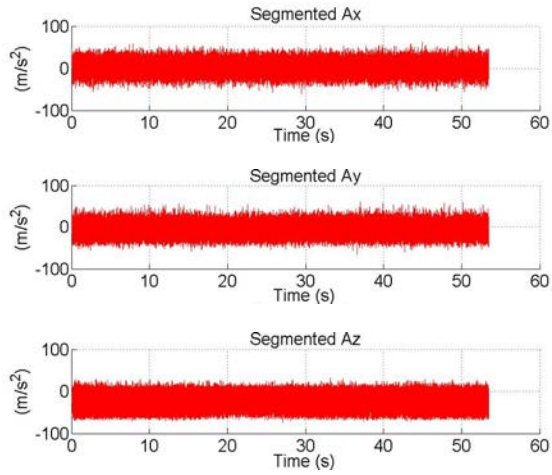

Fig. 9. Segmented A_x, A_y and A_z vibration acceleration signals.

The extracted sensor signal features can be employed to feed cognitive decision making support systems able to provide a diagnosis on tool wear state. The latter can be used for selecting appropriate corrective actions such as emergency stop of the machine, tool replacement (either automatic or manual) or adaptive change of the process parameters.

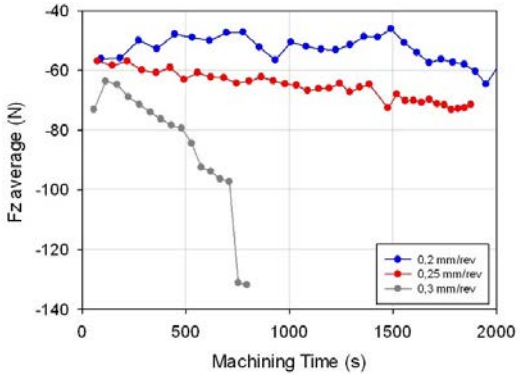

Fig. 10. Average of F_z cutting force component signal, F_{z_av}, vs machining time for f_1 = 0.2 mm/rev, f_2 = 0.25 mm/rev, f_3 = 0.3 mm/rev (v = 60 m/min, d = 0.5 mm).

4.3. Sensor signal features selection

The signal feature extraction procedure generated five features for each acquired signal. This large number of extracted features needs a proper selection method to identify the most relevant features for the tool wear monitoring scope. A statistical approach based on the calculation of the Pearson correlation coefficient was employed to evaluate the correlation between extracted features and tool wear conditions. The correlation coefficient, *r*, between a certain feature *x* and tool wear value *y* can be expressed as follows:

$$r^2 = \frac{\left(\sum_i \left(x_i - \bar{x}\right)\left(y_i - \bar{y}\right)\right)^2}{\sum_i \left(x_i - \bar{x}\right)^2 \sum_i \left(y_i - \bar{y}\right)^2} \quad (1)$$

It can be said that:
- if $0 < r < 0.3$, the correlation between the variables is weak;
- if $0.3 < r < 0.7$, the correlation is moderate;
- if $0.7 < r < 1$, the correlation is strong.

Based on the *r* value, only 8 out of all the extracted statistical features showed a strong correlation with tool wear: F_x average (F_{x_av}), F_y average (F_{y_av}), F_z average (F_{z_av}), AE_{RMS} average (AE_{RMS_av}), F_x skewness (F_{x_sk}), F_z skewness (F_{z_sk}), F_x kurtosis (F_{x_kurt}), F_z kurtosis (F_{z_kurt}).

Graphical analysis showed that the behaviour of the selected statistical sensor signal features and the behaviour of the tool wear development are very close. Fig. 10 illustrates the F_{z_av} feature behaviour for cutting tests at v = 60m/min, d = 0.5 mm with diverse feed rate values: f_1 = 0.2 mm/rev, f_2 = 0.25 mm/rev, f_3 = 0.3 mm/rev.

5. Artificial neural networks for tool wear curve reconstruction and generation

The selected statistical features were employed to construct sensor fusion feature pattern vectors (SFPVs) to be correlated with tool wear state through cognitive pattern recognition based on artificial neural networks (ANN) [9].

ANN paradigms were developed to accomplish two main objectives: (a) reconstruction of the missing points of a single tool wear curve obtained from several passes under a given turning condition; (b) generation of the entire tool wear curve for a given turning condition based on a training set consisting of sensor signal features and corresponding tool wear values measured for different turning conditions.

In both cases, three-layer cascade-forward backpropagation ANNs using the Levenberg-Marquardt optimization algorithm for training were setup, and an algorithm to train and test different numbers of hidden layer nodes was implemented.

Tool wear curve reconstruction

For each turning condition, ANNs were set up in order to reconstruct the complete tool wear curve based on the features extracted from the signal data relative to the consecutive turning passes carried out with the same turning condition.

The ANNs were fed with a set of 9-feature $SFPV_a$ constructed for each turning pass in a full turning test by combining the selected statistical signal features and the corresponding machining time (t), i.e. the time at which the turning pass was terminated.

$$SFPV_a = [F_{x\_av}, F_{y\_av}, F_{z\_av}, AE_{RMS\_av}, F_{x\_sk}, F_{z\_sk}, F_{x\_kurt}, F_{z\_kurt}, t]$$

Each $SFPV_a$ was associated to its matching flank wear value (VB_{max}) to create input-output vectors for ANN learning. For each turning condition, *n* input-output vectors (*n* = number of turning passes in a full turning test) were built to form the related ANN training set. ANN cross-validation was performed through the leave-k-out method with $k = 1$ [16].

According to the leave-k-out method, at each step, $k = 1$ $SFPV_a$ is removed in turn from the original set of *n* $SFPV_a$ and used for ANN testing while the remaining *n-k* $SFPV_a$ are used for training. This is repeated for all the *n* $SFPV_a$ and the overall pattern recognition performance is eventually estimated by combining the *n* recognition rates obtained.

Diverse configurations of ANNs using different numbers of hidden layer nodes, multiples of the number of input layer nodes (9, 18 and 27 nodes, respectively), were trained and tested to identify the best ANN configuration for the recognition of the maximum tool flank wear land, VB_{max}.

Tool wear curve generation

With the objective to generate the entire tool wear curve for a given turning condition, a different set of features was selected to construct the sensor fusion feature pattern vector $SFPV_b$ to be fed to the ANN. The new $SFPV_b$ is a 12-feature vector constructed by adding to $SFPV_a$ the cutting parameters, i.e. cutting speed, v, feed rate, f, and depth of cut, d.

$$SFPV_b = [F_{x\_av}, F_{y\_av}, F_{z\_av}, AE_{RMS\_av}, F_{x\_sk}, F_{z\_sk}, F_{x\_kurt}, F_{z\_kurt}, t, v, f, d]$$

In this case, a different leave-*k*-out procedure was applied, with *k* equal in turn to the number of passes of the turning condition to be tested: this means removing all the $SFPV_b$ and corresponding tool wear values of the given turning condition from the training set. Therefore, the training set consists only of $SFPV_b$ and corresponding tool wear values measured at turning conditions different from the one to be tested. In particular, surrounding cutting conditions were selected for training by fixing two of three cutting parameters and varying the last one. E.g., to generate the tool wear curve for $v_1 = 60$ m/min, $f_1 = 0.25$ mm/rev, $d_1 = 0.5$ mm, the $SFPV_b$ and corresponding tool wear values obtained for $v_2 = 60$ m/min, $f_2 = 0.20$ mm/rev, $d_2 = 0.5$ mm and for $v_3 = 60$ m/min, $f_3 = 0.30$ mm/rev, $d_3 = 0.5$ mm were used to train the ANN.

6. Results and discussion

The ANN based pattern recognition performance was estimated in terms of mean squared error, MSE, between the ANN predicted VB_{max} values and the measured VB_{max} values.

Table 3 reports the MSE values obtained from the ANN tool wear curve reconstruction for the experimental tests carried out at v = 60 m/min with various feed rate and depth of cut values. As it can be observed, very low MSE values between 0.00064 and 0.02275 were attained, providing an accurate tool wear curve reconstruction with ANN output values very close to the measured tool wear values. In most cases, the best performance was obtained with the 9-9-1 ANN configuration. In the other cases, it was obtained with the 9-27-1 ANN configuration (Fig. 11).

Table 3. Overall Mean Square Error (MSE) obtained by ANN tool wear reconstruction for all the turning tests carried out at v = 60 m/min.

	MSE		
	9 hidden nodes	18 hidden nodes	27 hidden nodes
60-0.30-1.0	0.00049	0.02098	0.00992
60-0.30-1.5	0.00225	0.06577	0.02998
60-0.25-1.0	0.01019	0.02903	0.01160
60-0.20-1.0	0.00495	0.02128	0.05334
60-0.30-0.5	0.04696	0.02275	0.02703
60-0.20-0.5	0.01651	0.01330	0.00524
60-0.25-0.5	0.00370	0.00064	0.00096
60-0.20-1.5	0.00518	0.02649	0.01499
60-0.25-1.5	0.00748	0.04195	0.03017

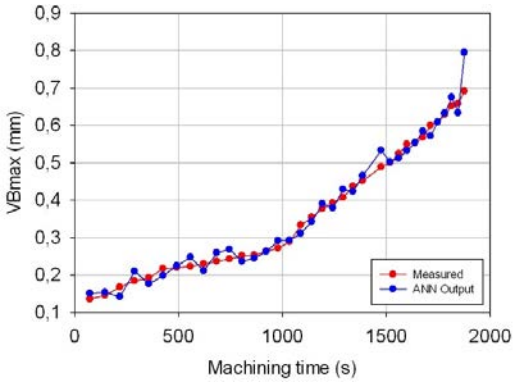

Fig. 11. ANN output vs measured VB_{max} for turning test at v = 60 m/min, f = 0.25 mm/rev, d = 0.5 mm. ANN configuration: 9-27-1. MSE = 0.00524.

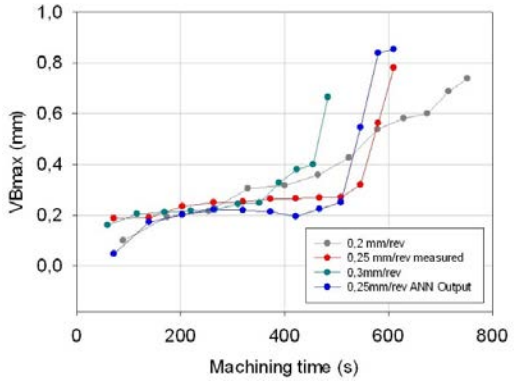

Fig. 12. ANN entire tool wear curve generation. The tool wear curve for v_1 = 60 m/min, f_1 = 0.25 mm/rev, d_1 = 1.5 mm is obtained using a training set comprising sensor signal features and corresponding tool wear values for v_2 = 60 m/min, f_2 = 0.20 mm/rev, d_2 = 1.5 mm and v_3 = 60 m/min, f_3 = 0.30 mm/rev, d_3 = 1.5 mm. ANN configuration: 12-24-1. MSE = 0.01373.

As regards the tool wear curve generated by training the ANN with $SFPV_b$ and corresponding tool wear values measured for different turning conditions, slightly higher MSE values between 0.00613 and 0.02683 were obtained, suggesting that this task is more challenging for the ANN. Fig. 12 shows the tool wear curve for turning with v_1 = 60 m/min, f_1 = 0.25 mm/rev, d_1 = 1.5, generated by the ANN trained with signal features and corresponding tool wear values for surrounding turning conditions. Although a higher MSE = 0.01373 was obtained in this case, the ANN is still able to satisfactorily provide the tool wear development and identify the critical moment at which the transition of the tool wear curve between second and third tool wear zone occurs.

This allows an accurate diagnosis on tool state that could be reliably implemented on-line. The ANN based diagnosis on tool state can be used for selecting appropriate corrective actions which can be directly fed to the machine tool numerical controller (e.g. for emergency halting or cutting parameters change) or suggested to the machine operator (e.g. for manual tool replacement operations).

7. Conclusions

An experimental testing campaign of dry turning on Ti6Al4V alloy bars was carried out with the aim to develop a cognitive sensor monitoring procedure for tool wear state diagnosis based on the acquisition and processing of cutting force, acoustic emission and vibration sensor signals.

The experimental tests showed that 70 m/min and 80 m/min cutting speeds result in extremely rapid tool wear and very low machining time and material removal per tool life. These phenomena are intensified with increasing feed rate and depth of cut values. Also in the case of v = 60 m/min, which appears as most suitable for dry turning of this difficult-to-machine alloy, tool wear monitoring appears necessary to deal with the rapid tool wear development.

The procedure developed for accurate diagnosis of tool wear state involved sensor signal feature extraction, selection and cognitive pattern recognition via ANN.

The latter provided accurate tool wear reconstruction and generation, with ANN output values very close to the measured tool wear values and MSE values < 0.02683.

This confirms the capability of the developed procedure to reliably carry out a diagnosis on tool wear state, which can be employed to support decision making for appropriate corrective actions on tool replacement, parameters change or process stop, which can be either directly fed to the machine tool numerical controller or suggested to the human operator.

Additional experimental turning tests will be performed to increase the training set for tool wear curve reconstruction and generation. Further experimental tests with the use of a vortex tube powered by compressed air as coolant will be carried out in order to extend tool life in turning of Ti6Al4V [15].

Acknowledgements

The Fraunhofer Joint Laboratory of Excellence on Advanced Production Technology (Fh-J_LEAPT Naples) at the Department of Chemical, Materials and Industrial Production Engineering, University of Naples Federico II, is gratefully acknowledged for its contribution and support to this research.

References

[1] Duflou JR, Sutherland JW, Dornfeld D, Herrmann C, Jeswiet J, Kara S, Hauschild M, Kellens K. Towards energy and resource efficient manufacturing: A processes and systems approach. CIRP Annals 2012; 61/2: 587-609.
[2] Donachie MJ Jr. Titanium and Titanium Alloys. American Society for Metals, Metals Park, Ohio 1983.
[3] Donachie, MJ Jr. Titanium – A Technical Guide. American Society for Metals, Metals Park, Ohio 1988.
[4] Ezugwu EO, Wang ZM. Titanium alloys and their machinability - a review. Journal of Materials Processing Technology 1997; 68: 262-274.
[5] Ginting A, Nouari M. Surface integrity of dry machined titanium alloys. Int. J. of Machine Tools & Manufacture 2009; 49: 325-332.
[6] Che-Haron CH, Jawaid A. The effect of machining on surface integrity of titanium alloy Ti6Al4V. J. of Mater. Proc. Techn. 2005; 166:188-192.
[7] Che-Haron CH. Tool life and surface integrity in turning titanium alloy. Journal of Materials Processing Technology 2001; 118: 231-237.
[8] Teti R, Jemielnak K, O'Donnell G, Dornfeld D. Advanced monitoring of machining operations. CIRP Annals 2010; 59/1: 717-739.
[9] Teti R. Advanced IT methods of signal processing and decision making for zero defect manufacturing in machining. ProcediaCIRP 2015;28:3-15
[10] Caggiano A, Perez R, Segreto T, Teti R. Xirouchakis P. Advanced Sensor Signal Feature Extraction and Pattern Recognition for Wire EDM Process Monitoring. Procedia CIRP 2016; 42: 34-39.
[11] Segreto T, Caggiano A, Teti R. Neuro-fuzzy System Implementation in Multiple Sensor Monitoring for Ni-Ti Alloy Machinability Evaluation. Procedia CIRP 2015; 37: 193-198.
[12] Quan Y, Zhoub M, Luo Z. On-Line Robust Identification of Tool Wear Via Multi-sensor NN fusion. Engineering Applications of Artificial Intelligence 1998; 11: 717-722.
[13] Balsamo V, Caggiano A, Jemielniak K, Kossakowska J, Nejman M, Teti R. Multi Sensor Signal Processing for Catastrophic Tool Failure Detection in Turning. Procedia CIRP 2016; 41: 939-944.
[14] Caggiano, A., Segreto, T., Teti, R., Cloud Manufacturing Framework for Smart Monitoring of Machining, Procedia CIRP 2016; 55: 248-253.
[15] Rubio EM, Agustina B, Marìn M, Bericua A. Cooling systems based on cold compressed air: a review of the applications in machining processes. Procedia Engineering 2015; 132: 413-418.
[16] Abe S. Pattern classification: neuro-fuzzy methods and their comparison, Springer-Verlag London, 2001.